TWMS J. App. and Eng. Math. V.14, N.2, 2024, pp. 801-815

FITTED COMPUTATIONAL METHOD FOR CONVECTION DOMINATED DIFFUSION EQUATIONS WITH SHIFT ARGUMENTS

MESFIN MEKURIA WOLDAREGAY[1], §

Abstract. A time dependent singularly perturbed convection diffusion equation involving shift parameters are considered. The terms containing the shifts are treated using Taylor series approximation up to second order terms. Classical numerical methods developed for solving regular problems fail to give good approximate solution and become unstable while applied for the considered problem. In this paper, numerical scheme is developed using θ-method for semi-discretizing in time derivative; in spatial discrtization fitted operator finite difference method is applied by inducing exponential fitting parameter. To accelerate the convergence of the scheme, Richardson extrapolation technique is applied in spatial discretization. Existence of unique discrete solution is guaranteed by establishing the discrete comparison principle. The proposed scheme is stable for all values of the perturbation parameter. A uniformly convergent solution is obtained by Richardson extrapolation method which provides second order accuracy under some condition. Test examples are considered for validating the theoretical results numerically.

Keywords: Exponentially fitted scheme, Richardson extrapolation, convection dominated, uniform convergence.

AMS Subject Classification: 65M06, 65M12, 65M15.

1. Introduction

A time dependent singularly perturbed differential difference equations (DDEs) model process for which the evaluation depend on the current state of the system and its past history. A number of model problems in science and engineering take the forms of time dependent singularly perturbed DDEs [31], to list few of them: the neuron variability model in computational neuroscience, model describing the motion of sunflower and optimal control theory problems. In general, classical numerical methods developed for regular problems fails to give good approximate solution for singularly perturbed problems, when the perturbation parameter approaches to zero [25].

Currently, scholars' are working on fitted numerical methods that converges uniformly for treating stationary and time dependent singularly perturbed problems [11]. There are essentially two strategies to design numerical schemes which gives small errors inside the boundary layer region. The first approach is the class of fitted mesh methods which

[1] Department of Applied Mathematics, Adama Science and Technology University, Adama, Ethiopia. e-mail: msfnmkr02@gmail.com; ORCID: https://orcid.org/ 0000-0002-6555-7534.

§ Manuscript received: February 20, 2022; accepted: May 29, 2022.

chooses a fine mesh in the boundary layer region and coarse mesh in outer layer region. A detail discussion in using fitted mesh methods can be found in [5, 7, 8, 18, 26] and the reference therein. The second approach is the fitted operator methods in which the mesh remains uniform and the difference schemes reflect the qualitative behaviour of the solution inside the boundary layer region.

In this article, numerical solution of time dependent singularly perturbed DDE is considered. The authors in [19, 20] treated stationary form of the considered problem using asymptotic method. Woldaregay and Duressa [30, 31, 32, 33] used different class of fitted FDM in spatial discretization for treating singularly perturbed problems. Kumar and Kumar [15, 16, 17] used a monotone Schwarz iterative method for the spatial discretization. Kumar and Kadalbajoo [14] used B-spline method on piecewise uniform mesh in space discretization. Gupta et al. [13] used midpoint upwind in the outer region and central finite difference method in the layer region for space discretization and by using the Richardson extrapolation method they increased the rate of convergence. Ramesh and Kadalbajoo [23] used upwind and midpoint upwind finite difference on Shishkin mesh for the spatial discretization. Bansal and Sharma in [1, 2, 3] applied a non standard FDM for the spatial discretization with different methods for temporal discretization.

However, The aforementioned schemes developed so far are less than linear order accurate. Numerical treatment of singularly perturbed problems needs improvement [12] and developing higher order numerical methods that coverages uniformly irrespective of the perturbation parameter is an active research area [27]. In this article, for treating time dependent singularly perturbed DDEs, we are interested to develop second order accurate numerical method that coverages uniformly irrespective of the perturbation parameter. The θ-method is used for the time derivative semi-discretization and fitted operator finite difference method for the spatial derivative discerization. Furthermore, we established the convergence analysis of the scheme. The proposed scheme works only for linear and one dimensional problems, for solving non-linear and higher dimensional problems one can use the techniques in [6, 21, 25].

Throughout this paper, the norm $\|.\|$ represents the maximum norm; the symbols N and M are denoted respectively for the number of mesh grids in spacial and temporal discretization; the constant C is denoted for positive constant independent of ε and N.

2. Statement of the problem

On the domain $D = \Omega \times \Lambda = (0,1) \times (0,T]$ with the boundary $\partial D = \bar{D} \backslash D$, a class of time dependent convection dominated DDE is given by

$$\begin{cases} u_t - \varepsilon^2 u_{xx} + a(x)u_x + b(x)u(x-\delta,t) + c(x)u(x,t) + d(x)u(x+\eta,t) = g(x,t), \\ u(x,0) = u_0(x), \quad x \in \bar{\Omega}, \\ u(x,t) = \phi_l(x,t), \ -\delta \le x \le 0, \ t \in \Lambda, \\ u(x,t) = \phi_r(x,t), \ 1 \le x \le 1+\eta, \ t \in \ \Lambda, \end{cases} \tag{1}$$

where δ and η are the negative and positive shift parameters and $\varepsilon \in (0,1]$ is the perturbation parameter. We assumed that the functions $a, b, c, d, g, u_0, \phi_l$ and ϕ_r are smooth and bounded. Furthermore, for the existence of boundary layer in the solution of (1), we assumed that

$$b(x) + c(x) + d(x) \ge \Upsilon > 0, \tag{2}$$

for some constant Υ.

2.1. **Estimates and bounds of the solution.** For the case $\delta, \eta < \varepsilon$, the terms with the shifts $u(x-\delta, t)$ and $u(x+\eta, t)$ are approximated using Taylor's series approximation [29]. So, equation (1) simplifies to

$$\begin{cases} u_t - c_\varepsilon u_{xx} + \nu(x)u_x + \kappa(x)u(x,t) = g(x,t), (x,t) \in D, \\ u(x,0) = u_0(x), \ x \in \bar{\Omega}, \\ u(0,t) = \phi_l(0,t), \ \ t \in \Lambda, \\ u(1,t) = \phi_r(1,t), \ t \in \Lambda. \end{cases} \tag{3}$$

where $c_\varepsilon := \varepsilon^2 - (\delta^2/2)b - (\eta^2/2)d$, $\nu(x) := a(x) - \delta b(x) + \eta d(x)$ and $\kappa(x) := b(x) + c(x) + d(x)$ for b and c are lower bounds of $b(x)$ and $c(x)$.

The solution exhibits a boundary layer and the position of the layer depends on the sign of $\nu(x) = a(x) - \delta b(x) + \eta d(x)$. If $\nu(x) > 0$, right boundary layer exists and if $\nu(x) < 0$, left boundary layer exists and for the case $\nu(x)$ changes sign, shock layer exists inside the domain [23]. The boundary layer is maintained for sufficiently small shift parameters $\delta, \eta < c_\varepsilon$ [13].

Lemma 2.1. *Let $u_0 \in C^2[0,1]$, and $\phi_l, \phi_r \in C^1[0,T]$, we impose the corner compatibility conditions*

$$\begin{cases} u_0(0) = \phi_l(0,0), \\ u_0(1) = \phi_r(1,0), \end{cases} \tag{4}$$

and

$$\begin{cases} \frac{\partial \phi_l(0,0)}{\partial t} - c_\varepsilon \frac{\partial^2 u_0(0)}{\partial x^2} + \nu(0)\frac{\partial u_0(0)}{\partial x} + \kappa(0)u_0(0) = g(0,0), \\ \frac{\partial \phi_r(1,0)}{\partial t} - c_\varepsilon \frac{\partial^2 u_0(1)}{\partial x^2} + \nu(1)\frac{\partial u_0(1)}{\partial x} + \kappa(1)u_0(1) = g(1,0), \end{cases} \tag{5}$$

so that the data matches at the two corners $(0,0)$ and $(1,0)$. Since $\nu(x), \kappa(x)$ and $g(x,t)$ are continuous functions on the domain D, (3) has unique solution $u \in C^2(D)$.

If we set $c_\varepsilon = 0$ in the problem (3), it is called reduced problem and given as

$$\begin{cases} u^0_t + \nu(x)u^0_x + \kappa(x)u^0(x,t) = g(x,t), \ (x,t) \in D, \\ u^0(x,0) = u_0(x), \ x \in \bar{\Omega}, \\ u^0(0,t) = \phi_l(0,t), \ t \in \bar{\Lambda}. \end{cases} \tag{6}$$

The problem in (6) is a first order hyperbolic PDE with given data along the sides $x = 0$ and $t = 0$ of $\bar{D}$. As $c_\varepsilon \to 0$, the solution $u(x,t)$ of (3) becomes very close to the solution $u^0(x,t)$ of (6). For the sack of simplicity we denote the differential operator in (3) as $\mathcal{L}u(x,t) = u_t - c_\varepsilon u_{xx} + \nu(x)u_x + \kappa(x)u(x,t)$.

Lemma 2.2 (The maximum principle [4])**.** *Let u be a sufficiently smooth function defined on D which satisfies $u(x,t) \geq 0, \ (x,t) \in \partial D$. Then, $\mathcal{L}u(x,t) \geq 0, \ (x,t) \in D$ implies that $u(x,t) \geq 0, \ (x,t) \in \bar{D}$.*

Lemma 2.3. *The solution $u(x,t)$ of (3) satisfies the bound*

$$|u(x,t)| \leq \frac{\|\mathcal{L}u\|}{\kappa} + \max\{|u_0(x)|, |\phi_l(0,t)|, |\phi_r(1,t)|\}, \tag{7}$$

where κ is the lower bound of $\kappa(x)$.

Proof. Let $\mathcal{F} = \frac{\|\mathcal{L}u\|}{\kappa} + \max\{|u_0(x)|, |\phi_l(0,t)|, |\phi_r(1,t)|\}$, construct a barrier function $\vartheta^{\pm}(x,t) = \mathcal{F} \pm u(x,t)$. The function $\vartheta^{\pm}(x,t)$ satisfies the bound at the initial value as

$$\vartheta^{\pm}(x,0) = \mathcal{F} \pm u(x,0) = \frac{\|\mathcal{L}u\|}{\kappa} + \max\{|u_0(x)|, |\phi_l(0,t)|, |\phi_r(1,t)|\} \pm u(x,0) \geq 0.$$

On the boundaries, we have

$$\vartheta^{\pm}(0,t) = \mathcal{F} \pm u(0,t) = \frac{\|\mathcal{L}u\|}{\kappa} + \max\{|u_0(x)|, |\phi_l(0,t)|, |\phi_r(1,t)|\} \pm u(0,t) \geq 0.$$

$$\vartheta^{\pm}(1,t) = \mathcal{F} \pm u(1,t) = \frac{\|\mathcal{L}u\|}{\kappa} + \max\{|u_0(x)|, |\phi_l(0,t)|, |\phi_r(1,t)|\} \pm u(1,t) \geq 0,$$

and on the domain D, we have

$$\begin{aligned}\mathcal{L}\vartheta^{\pm}(x,t) =& \vartheta^{\pm}_t(x,t) - c_\varepsilon \vartheta^{\pm}_{xx}(x,t) + \nu(x)\vartheta^{\pm}_x(x,t) + \kappa(x)\vartheta^{\pm}(x,t)\\ =& \frac{\partial}{\partial t}\big(\mathcal{F} \pm u(x,t)\big) - c_\varepsilon \frac{\partial^2}{\partial x^2}\big(\mathcal{F} \pm u(x,t)\big) + \nu(x)\frac{\partial}{\partial x}\big(\mathcal{F} \pm u(x,t)\big)\\ &+ \kappa(x)\big(\mathcal{F} \pm u(x,t)\big),\ \textit{since } \mathcal{F} \textit{ is constant}\\ =& \kappa(x)\big(\frac{\|\mathcal{L}u\|}{\kappa} + \max\{|u_0(x)|, |\phi_l(0,t)|, |\phi_r(1,t)|\}\big) \pm \mathcal{L}u(x,t)\\ \geq& 0,\ \ \textit{since } \kappa(x) \geq \kappa > 0.\end{aligned}$$

Hence, we obtain, $\vartheta^{\pm}(x,t) \geq 0,\ (x,t) \in \bar{D}$ by the maximum principle. □

Lemma 2.4. *Derivatives of the solution $u(x,t)$ of (3) with respect to x and t satisfies the bounds*

$$\begin{cases} \left|\frac{\partial^k u(x,t)}{\partial x^k}\right| \leq C\big(1 + c_\varepsilon^{-k} \exp\big(-\frac{\nu(1-x)}{c_\varepsilon}\big)\big),\ (x,t) \in \bar{D},\ 0 \leq k \leq 4.\\ \left|\frac{\partial^l u(x,t)}{\partial t^l}\right| \leq C,\ (x,t) \in \bar{D},\ l = 0,1,2, \end{cases} \tag{8}$$

where ν is lower bound of $\nu(x)$.

Proof. See in [2]. □

3. The discrete scheme

3.1. **Time direction discretization.** By sub-dividing $[0,T]$ as $t_0 = 0,\ t_j = j\Delta t, j = 0,1,2,...,M-1$, where $\Delta t = \frac{T}{M-1}$ into $M-1$ elements; the continuous problem (3) is semi-discretized using θ-method. For the case $\theta = 1$, the scheme becomes implicit Euler method and for $\theta = \frac{1}{2}$ it become Crank Nicolson method which is second order consistent. In general, stable numerical scheme is obtained for $\frac{1}{2} \leq \theta \leq 1$ [28]. We denote $U^{j+1}(x)$ for the approximation of $u(x,t_{j+1})$ at the $(j+1)th$ level discretization.

In this discretization, we obtain a system of singularly perturbed BVPs of the form

$$\begin{cases} (1 + \Delta t\theta\mathcal{L}^{\Delta t})U^{j+1}(x) = & (1 - (1-\theta)\Delta t\mathcal{L}^{\Delta t})U^j(x) + \Delta t(\theta g(x,t_{j+1})\\ & +(1-\theta)\Delta t g(x,t_j)),\ x \in \Omega,\\ U^{j+1}(0) = \phi_l(0,t_{j+1}), & \\ U^{j+1}(1) = \phi_r(1,t_{j+1}), & \end{cases} \tag{9}$$

for $j = 0,1,2,...,M-1$, where $\mathcal{L}^{\Delta t} = -c_\varepsilon \frac{d^2}{dx^2} + \nu(x)\frac{d}{dx} + \kappa(x)$.

In the next few lemmas, we discuss the stability analysis and truncation error bound of the semi-discrete scheme.

Lemma 3.1. *On the domain $\bar{\Omega}$, let $U^{j+1}(x)$ be sufficiently smooth function. If $U^{j+1}(0) \geq 0$, $U^{j+1}(1) \geq 0$, then $(1 + \theta\Delta t\mathcal{L}^{\Delta t})U^{j+1}(x) \geq 0, x \in \Omega$, implies that $U^{j+1}(x) \geq 0, x \in \bar{\Omega}$.*

Proof. Let $x^* \in \bar{\Omega}$ be such that $U^{j+1}(x^*) = \min_{x\in\bar{\Omega}} U^{j+1}(x)$. Suppose that $U^{j+1}(x^*) < 0$. From our assumption, we have that $x^* \neq 0, 1$ giving that $x^* \in (0,1)$. Since $U^{j+1}(x^*) = \min_{x\in\bar{\Omega}} U^{j+1}(x)$, from the extrema values property we obtain $U^{j+1}_x(x^*) = 0$ and $U^{j+1}_{xx}(x^*) \geq 0$, gives that $(1+\theta\Delta t\mathcal{L}^{\Delta t})U^{j+1}(x^*) < 0$, which is contradiction to $(1+\theta\Delta t\mathcal{L}^{\Delta t})U^{j+1}(x^*) \geq$

$0,\ x \in \Omega$. Hence, $U^{j+1}(x) \geq 0,\ x \in \bar{\Omega}$. The operator $(1+\theta\Delta t\mathcal{L}^{\Delta t})$ satisfies the semi-discrete maximum principle. Consecutively we obtain

$$\|(1+\theta\Delta t\mathcal{L}^{\Delta t})^{-1}\| \leq \frac{1}{1+\theta\Delta t\kappa}. \tag{10}$$

□

Lemma 3.2 (Global error estimate.)**.** *The temporal discretization error up to t_{j+1} time step is bounded as*

$$\|E_{j+1}\| \leq \begin{cases} C(\Delta t),\ \frac{1}{2} < \theta \leq 1, \\ C(\Delta t)^2,\ \theta = \frac{1}{2}, \end{cases} \quad j = 1,2,...,M-1. \tag{11}$$

Lemma 3.3. *Let $U^{j+1}(x)$ be solution of (9), then it satisfies the following bound*

$$|U^{j+1}(x)| \leq \frac{\|(1+\Delta t\theta\mathcal{L}^{\Delta t})U_{j+1}\|}{1+\Delta t\theta\kappa} + \max\{|\phi_l(0,t_{j+1})|, |\phi_r(1,t_{j+1})|\}. \tag{12}$$

Proof. Let us construct barrier functions $\pi_{\pm}^{j+1}(x)$ as $\pi_{\pm}^{j+1}(x) = \mathcal{F}^{j+1} \pm U^{j+1}(x)$ where $\mathcal{F}^{j+1} = \frac{\|(1+\Delta t\theta\mathcal{L}^{\Delta t})U_{j+1}\|}{1+\Delta t\theta\kappa} + \max\{|\phi_l(0,t_{j+1})|, |\phi_r(1,t_{j+1})|\}$. We need to show the barrier function satisfies the maximum principle i.e. If $\pi_{\pm}^{j+1}(0) \geq 0,\ \pi_{\pm}^{j+1}(1) \geq 0$ in order to show $(1+\Delta t\theta\mathcal{L}^{\Delta t})\pi_{\pm}^{j+1}(x) \geq 0, x \in \Omega$ then, $\pi_{\pm}^{j+1}(x) \geq 0, x \in \bar{\Omega}$. One can show that $\pi_{\pm}^{j+1}(0) \geq 0$, and $\pi_{\pm}^{j+1}(1) \geq 0$ then, we show

$$\begin{aligned}
&(1+\Delta t\theta\mathcal{L}^{\Delta t})\pi_{\pm}^{j+1}(x) \\
&= \pi_{\pm}^{j+1}(x) + \Delta t\theta\big(-c_\varepsilon\frac{d^2}{dx^2} + \nu(x)\frac{d}{dx} + \kappa(x)\big)\pi_{\pm}^{j+1}(x) \\
&= (1+\Delta t\theta\kappa(x))\big(\frac{\|(1+\Delta t\theta\mathcal{L}^{\Delta t})U_{j+1}\|}{1+\Delta t\theta\kappa} + \max\{|\phi_l(0,t_{j+1})|, |\phi_r(1,t_{j+1})|\}\big) \\
&\quad \pm (1+\Delta t\theta\mathcal{L}^{\Delta t})U_{j+1}(x) \geq 0,\ \text{since } \kappa(x) \geq \kappa.
\end{aligned}$$

We conclude that $(1+\Delta t\theta\mathcal{L}^{\Delta t})\pi_{\pm}^{j+1}(x) \geq 0$. So, using the semi-discrete maximum principle, we have that $\pi_{\pm}^{j+1}(x) \geq 0,\ x \in \bar{\Omega}$. Hence the required bound follows □

Lemma 3.4. *The derivatives of the solution of the boundary value problem in (9) satisfy the bound*

$$\left|\frac{d^k}{dx^k}U^{j+1}(x)\right| \leq C\big(1 + c_\varepsilon^{-k}e^{-\frac{\nu(1-x)}{c_\varepsilon}}\big),\ x \in \bar{\Omega},\ k = 0,1,2,3,4. \tag{13}$$

where ν is lower bound of $\nu(x)$.

3.2. **Discretization in spatial direction.** For the spatial domain discretization, we use uniform mesh as $x_0 = 0, x_i = ih, x_N = 1, i = 0,1,2,...,N$, where $h = \frac{1}{N}$. Exponentially fitted operator FDM will be applied for treating the resulted boundary value problems. To apply the spatial discretization, we first find the exponential fitting parameter for any linear BVP.

3.2.1. *The fitting parameter.* 'To obtain the numerical solution of (9), we use the technique in the theory of asymptotic method for solving singularly perturbed BVPs. Since the boundary layer is on the right side of the domain, from the theory of singular perturbations problems [22] the zeroth order asymptotic solution of the singularly perturbed BVPs of the form'

$$\begin{cases} -c_\varepsilon u''(x) + \nu(x)u'(x) + \kappa(x)u(x) = g(x), x \in (0,1), \\ u(0) = \alpha,\ \ u(1) = \beta, \end{cases} \tag{14}$$

is given by

$$u(x) = u_0(x) + (\beta - u_0(1))e^{(-\frac{\nu(1)(1-x)}{c_\varepsilon})}, \quad (15)$$

where u_0 is the solution of the reduced problem. On the mesh points $x_0 = 0, x_i = ih, x_N = 1, i = 0, 1, 2, ..., N$, where $h = \frac{1}{N}$, evaluating the result in (15) at x_i gives

$$u(ih) = u_0(0) + (\beta - u_0(1))e^{(-\nu(1)(1/c_\varepsilon - i\rho))}, \quad (16)$$

where $\rho = \frac{h}{c_\varepsilon}$. For a mesh function u_i, we define the following difference operators $D^+z_i = \frac{z_{i+1}-z_i}{h}$, $D^-z_i = \frac{z_i - z_{i-1}}{h}$, $D^0 z_i = \frac{z_{i+1}-z_{i-1}}{2h}$, and $D^+D^-z_i = \frac{z_{i+1}-2z_i+z_{i-1}}{h^2}$.

We overcome the effect of the perturbation parameter by multiplying exponentially fitting parameter $\sigma(\rho)$ on the diffusion part of the problem. Applying the central finite difference method it takes the form

$$-c_\varepsilon\sigma(\rho)D^+D^-u(x_i) + \nu(x_i)D^0u(x_i) + \kappa(x_i)u(x_i) = g(x_i). \quad (17)$$

Multiplying (17) by h and considering h is small and truncating the term $h(g(x_i) - \kappa(x_i)u(x_i))$ to zero gives

$$\frac{\sigma(\rho)}{\rho}(u_{i-1} - 2u_i + u_{i+1}) + \frac{\nu(x_i)}{2}(u_{i+1} - u_{i-1}) = 0. \quad (18)$$

From (16), we have

$$u_{i\pm1} = u_0(0) + (\beta - u_0(1))e^{(-\nu(1)(1/\varepsilon-(i\pm1)\rho))}. \quad (19)$$

Substituting (19) into (18) and simplifying, the fitting parameter is obtained as

$$\sigma(\rho) = \frac{\rho\nu(x_i)}{2}\coth\big(\frac{\rho\nu(1)}{2}\big). \quad (20)$$

Using the difference operators into (9) and applying the exponential fitting parameter in (20), for $i = 1, 2, ..., N-1$, the fully discrete scheme obtained as

$$(1 + \Delta t\theta\mathcal{L}^{\Delta t,h})U_i^{j+1} = (1 - (1-\theta)\Delta t\theta\mathcal{L}^{\Delta t,h})U_i^j + \Delta t(\theta g(x_i, t_{j+1}) + (1-\theta)g(x_i, t_j)), \quad (21)$$

where $\mathcal{L}^{\Delta t,h}U_i^{j+1} = \sigma(\rho)c_\varepsilon D^+D^-U_i^{j+1} + \nu(x_i)D^0U_i^{j+1} + \kappa(x_i)U_i^{j+1}$.

We rewrite the scheme in (21), explicitly for $i = 1, 2, ..., N-1$, as

$$\begin{aligned} r_i^-U_{i-1}^{j+1} + r_i^cU_i^{j+1} + r_i^+U_{i+1}^{j+1} =& s_i^-U_{i-1}^j + s_i^cU_i^j + s_i^+U_{i+1}^j \\ &+ \Delta t(\theta g(x_i, t_{j+1}) + (1-\theta)g(x_i, t_j)) \end{aligned}$$

where

$$\begin{aligned} r_i^- &= -\Delta t\theta\big(\tfrac{c_\varepsilon\sigma(\rho)}{h^2} - \tfrac{\nu(x_i)}{2h}\big), & s_i^- &= -(1-\theta)\Delta t\big(\tfrac{c_\varepsilon\sigma(\rho)}{h^2} + \tfrac{\nu(x_i)}{2h}\big), \\ r_i^c &= 2\Delta t\theta\big(\tfrac{c_\varepsilon\sigma(\rho)}{h^2} + \kappa(x_i)\big) + 1, & s_i^c &= 2(1-\theta)\Delta t\big(\tfrac{c_\varepsilon\sigma(\rho)}{h^2} + \kappa(x_i)\big) + 1, \\ r_i^+ &= -\Delta t\theta\big(\tfrac{c_\varepsilon\sigma(\rho)}{h^2} - \tfrac{\nu(x_i)}{2h}\big), & s_i^+ &= -(1-\theta)\Delta t\big(\tfrac{c_\varepsilon\sigma(\rho)}{h^2} - \tfrac{\nu(x_i)}{2h}\big). \end{aligned}$$

3.3. **Stability analysis.** First, we need to prove the discrete comparison principle for the scheme in (21).

Lemma 3.5. *there exists a comparison function V_i^{j+1} such that if $U_0^{j+1} \leq V_0^{j+1}$, $U_N^{j+1} \leq V_N^{j+1}$ and $(1+\theta\Delta t\mathcal{L}^{h,\Delta t})U_i^{j+1} \leq (1+\theta\Delta t\mathcal{L}^{h,\Delta t})V_i^{j+1}$, $i = 1, 2, ..., N-1$ then $U_i^{j+1} \leq V_i^{j+1}$, $i = 0, 1, 2, ..., N$.*

Proof. Refer from [31]. □

The existence of unique discrete solution of the scheme is guaranteed by Lemma 3.5.

Lemma 3.6. *Let* $V_i^{j+1} = 1 + x_i, i = 0, 1, 2, ..., N$ *be monotone a mesh function. Then there exists a constant* C *such that* $(1 + \theta\Delta t\mathcal{L}^{h,\Delta t})V_i^{j+1} \geq C, i = 1, 2, ..., N-1$.

Proof. The proof is simple forward computation. □

Lemma 3.7. *The solution* U_i^{j+1} *of (21) satisfies the following bound*

$$|U_i^{j+1}| \leq \frac{\|(1 + \Delta t\theta\mathcal{L}^{h,\Delta t})U_i^{j+1}\|}{1 + \Delta t\theta\kappa} + \max\big\{|\phi_l(0, t_{j+1})|, |\phi_r(1, t_{j+1})|\big\}. \tag{22}$$

Proof. Let us construct a barrier function $\pi^{\pm}_{i,j+1}$ as $\pi^{\pm}_{i,j+1} = \mathcal{F}_i^{j+1} \pm U_i^{j+1}$ where $\mathcal{F}_i^{j+1} = \frac{\|(1+\Delta t\theta\mathcal{L}^{h,\Delta t})U_i^{j+1}\|}{1+\Delta t\theta\kappa} + \max\big\{|\phi_l(0, t_{j+1})|, |\phi_r(1, t_{j+1})|\big\}$. Then, we can show that $\pi^{\pm}_{0,j+1} \geq 0$ and $\pi^{\pm}_{N,j+1} \geq 0$. Then

$$\begin{aligned}(1 + \Delta t\theta\mathcal{L}^{h,\Delta t})\pi^{\pm}_{i,j+1} =& \pi^{\pm}_{i,j+1} + \Delta t\theta\big(-c_\varepsilon\frac{d^2}{dx^2} + \nu(x_i)\frac{d}{dx} + \kappa(x_i)\big)\pi^{\pm}_{i,j+1}\\ =& \frac{\|(1 + \Delta t\theta\mathcal{L}^{h,\Delta t})U_i^{j+1}\|}{1 + \Delta t\theta\kappa} + \max\big\{|\phi_l(0, t_{j+1})|, |\phi_r(1, t_{j+1})|\big\}\\ &\pm U_i^{j+1} + (1 + \Delta t\theta\kappa(x_i))\big[\frac{\|(1 + \Delta t\theta\mathcal{L}^{h,\Delta t})U_i^{j+1}\|}{1 + \Delta t\theta\kappa}\\ &+ \max\big\{|\phi_l(0, t_{j+1})|, |\phi_r(1, t_{j+1})|\big\} \pm U_i^{j+1}\big] \geq 0.\end{aligned}$$

Using the result in Lemma 3.5, we obtain $\pi^{\pm}_{i,j+1} \geq 0$, for $i = 0, 1, 2, ..., N$. □

Lemma 3.8. *If* V_i^{j+1} *be any mesh function such that* $V_0^{j+1} = V_N^{j+1} = 0$. *Then*

$$|V_i^{j+1}| \leq \frac{\|\mathcal{L}^{h,\Delta t}V_k^{j+1}\|}{1 + \Delta t\theta\kappa}.$$

Lemma 3.9. [31] *For* $c_\varepsilon \to 0$, *and for fixed* N, *we obtain*

$$\lim_{c_\varepsilon\to 0}\max_{1\leq i\leq N-1}\frac{e^{(\frac{-\nu x_i}{c_\varepsilon})}}{c_\varepsilon^m} = 0,\ \lim_{c_\varepsilon\to 0}\max_{1\leq i\leq N-1}\frac{e^{(\frac{-\nu(1-x_i)}{c_\varepsilon})}}{c_\varepsilon^m} = 0,\ m = 1, 2, 3, ... \tag{23}$$

Let C_1 and C_2 be constants. For all $y > 0$, we have $C_1\frac{y^2}{y+1} \leq y\coth(y) - 1 \leq C_2\frac{y^2}{y+1}$. So, for $\rho = \frac{h}{c_\varepsilon}$, we have

$$c_\varepsilon\big[\nu(x_i)\frac{\rho}{2}\coth\big(\nu(1)\frac{\rho}{2}\big) - 1\big] \leq \frac{h^2}{h + c_\varepsilon}. \tag{24}$$

In the proof of the following theorem, we use the result in (24).

Theorem 3.1. *The discrete scheme in (21) satisfies the truncation error bound*

$$\big|(1 + \Delta t\theta\mathcal{L}^{h,\Delta t})(U^{j+1}(x_i) - U_i^{j+1})\big| \leq \frac{Ch^2}{h + c_\varepsilon}\big(1 + c_\varepsilon^{-3}e^{(-\frac{\nu(1-x_i)}{c_\varepsilon})}\big). \tag{25}$$

Proof. Let us consider the truncation error

$$\begin{aligned}
|(1+\Delta t\theta\mathcal{L}^{h,\Delta t})(U^{j+1}(x_i)-U_i^{j+1})| =& \,\big|\, c_\varepsilon\big(\frac{d^2}{dx^2}-\sigma(\rho)D^+D^-\big)U^{j+1}(x_i)\\
&+\nu(x_i)\big(\frac{d}{dx}-D^0\big)U^{j+1}(x_i)\,\big|\\
\le& \,\big|\, c_\varepsilon\big[\nu(x_i)\frac{\rho}{2}\coth\big(\nu(1)\frac{\rho}{2}\big)-1\big]D^+D^-U^{j+1}(x_i)\,\big|\\
&+\,\big|\, c_\varepsilon\big(\frac{d^2}{dx^2}-D^+D^-\big)U^{j+1}(x_i)\,\big|\\
&+\,\big|\,\nu(x_i)\big(\frac{d}{dx}-D^0\big)U^{j+1}(x_i)\,\big|
\end{aligned}$$

since $\sigma(\rho)=\nu(x_i)\frac{\rho}{2}\coth\big(\nu(1)\frac{\rho}{2}\big)$. Using the results in (24) into (3.3) gives

$$\begin{aligned}
|(1+\Delta t\theta\mathcal{L}^{h,\Delta t})(U^{j+1}(x_i)-U_i^{j+1})| \le& \frac{Ch^2}{h+c_\varepsilon}\,\big|\,U_{xx}^{j+1}(x_i)\,\big|\,+Ch^2[c_\varepsilon\,\big|\,U_{xxxx}^{j+1}(x_i)\,\big|\\
&+\,\big|\,U_{xxx}^{j+1}(x_i)\,\big|\,].
\end{aligned}\tag{26}$$

Using the results in Lemma 3.4, we obtain

$$\begin{aligned}
&|(1+\Delta t\theta\mathcal{L}^{h,\Delta t})(U^{j+1}(x_i)-U_i^{j+1})|\\
\le&\frac{Ch^2}{h+c_\varepsilon}\big(1+c_\varepsilon^{-2}e^{(-\frac{\nu(1-x_i)}{c_\varepsilon})}\big)+Ch^2\big[c_\varepsilon\big(1+c_\varepsilon^{-4}e^{(-\frac{\nu(1-x_i)}{c_\varepsilon})}\big)+\big(1+c_\varepsilon^{-3}e^{(-\frac{\nu(1-x_i)}{c_\varepsilon})}\big)\big]\\
\le&\frac{Ch^2}{h+c_\varepsilon}\big(1+c_\varepsilon^{-2}e^{(-\frac{\nu(1-x_i)}{c_\varepsilon})}\big)+Ch^2\big[\big(c_\varepsilon+c_\varepsilon^{-3}e^{(-\frac{\nu(1-x_i)}{c_\varepsilon})}\big)\\
&+\big(1+c_\varepsilon^{-3}\exp(-\frac{\nu(1-x_i)}{c_\varepsilon})\big)\big]\\
\le&\frac{Ch^2}{h+c_\varepsilon}\big(1+c_\varepsilon^{-3}e^{(-\frac{\nu(1-x_i)}{c_\varepsilon})}\big),\ \text{since } c_\varepsilon^{-3}\ge c_\varepsilon^{-2}.
\end{aligned}$$

□

Using the results in Lemma 3.9, gives $|(1+\Delta t\theta\mathcal{L}^{h,\Delta t})(U^{j+1}(x_i)-U_i^{j+1})|\le\frac{Ch^2}{h+c_\varepsilon}, \forall c_\varepsilon>0$. Hence, using the discrete comparison principle in Lemma 3.5, we obtain

$$\big|\,U^{j+1}(x_i)-U_i^{j+1}\,\big|\,\le\frac{Ch^2}{h+c_\varepsilon}\le Ch. \tag{27}$$

3.4. **Richardson extrapolation.** Here, we use the Richardson extrapolation to accelerate the convergence of the scheme in spatial direction. One can find the detail derivation of the Richardson extrapolation in [8, 9]. From (27) we have

$$U_{j+1}(x_i)-U_i^{j+1}\approx Ch+O(h^2), \tag{28}$$

where $U_{j+1}(x_i)$ and U_i^{j+1} are exact and approximate solutions respectively. The truncation error in the spatial approximation becomes

$$U_{j+1}(x_i)-\tilde{U}_i^{j+1}\approx Ch^2+O(h^3), \tag{29}$$

where $\tilde{U}_i^{j+1}=2U_{i,2N}^{j+1}-U_i^{j+1}$. Here, $U_{i,2N}^{j+1}$ is denoted for the approximate solution on $2N$ number of mesh points by including the mid points $x_{i+1/2}=\frac{x_i+x_{i+1}}{2}$.

Theorem 3.2. *Let $u(x_i, t_{j+1})$ and U_i^{j+1} be respectively the solution of (3) and solution by the proposed scheme in (29) on discretized domain. Then, the following error estimate holds*

$$\sup_{0<c_\varepsilon\leq 1} \|u(x_i, t_{j+1}) - \tilde{U}_i^{j+1}\| \leq \begin{cases} C(h^2 + (\Delta t)), & \frac{1}{2} < \theta \leq 1, \\ C(h^2 + (\Delta t)^2), & \theta = \frac{1}{2}. \end{cases} \tag{30}$$

Proof. Immediate result from (27) and (11) and the bounded of the solution gives the required bound. □

4. Numerical examples and results

We take numerical examples that exhibit boundary layer behavior. For the considered examples, the exact solutions are not known.

Example 4.1. *We take the example in* [32]*, where $a(x) = 2 - x^2, \alpha(x) = 2, \beta(x) = x - 3, \omega(x) = 1$ and $g(x,t) = 10t^2e^{-t}x(1-x)$ with the initial condition $u_0(x) = 0$ and the boundary conditions $\phi(x,t) = 0$, and $\psi(x,t) = 0$, for $T = 3$.*

Example 4.2. *We take the example in* [32]*, where $a(x) = 2 - x^2, \alpha(x) = 1 + x, \beta(x) = 1 + x^2 + \cos(\pi x), \omega(x) = 3$ and $g(x,t) = \sin(\pi x)$ with the initial condition $u_0(x) = 0$ and the boundary conditions $\phi(x,t) = 0$, and $\psi(x,t) = 0$, for $T = 3$.*

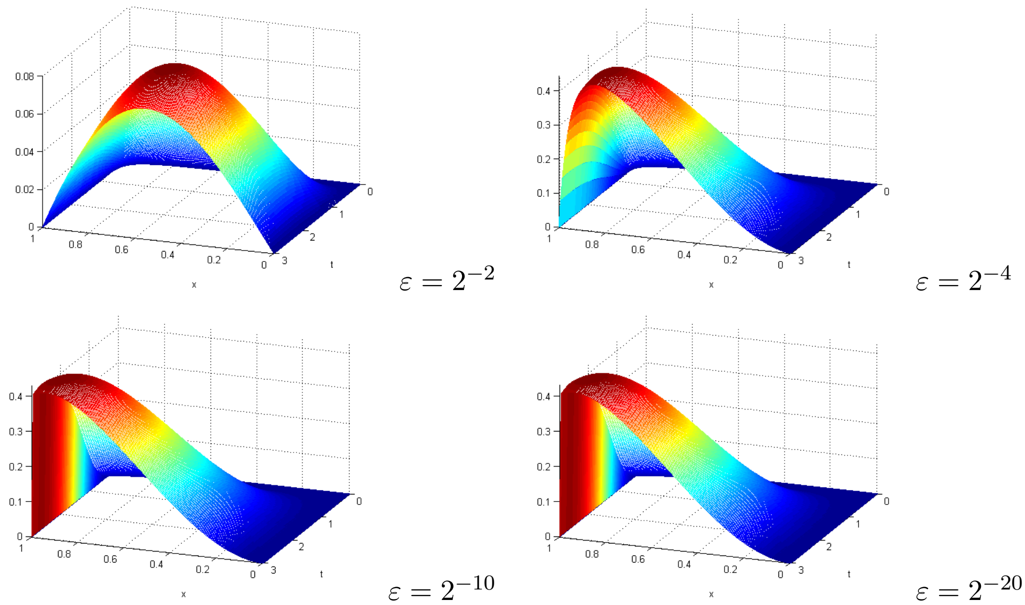

Figure 1. Boundary layer formation of the computed solution of Example 4.1.

For the considered examples the exact solution are not known. So, we use double mesh techniques for computing the maximum absolute error $(E_{\varepsilon,\delta}^{N,M})$. The maximum absolute error is calculated using the formula

$$E_{\varepsilon,\delta,\eta}^{N,M} = \max_{i,j} \left| U_{i,N}^{j,M} - \tilde{U}_{i,2N}^{j,2M} \right|,$$

where $U_{i,N}^{j,M}$ is the computed solution on N, M number of mesh points and $U_{i,2N}^{j,2M}$ is the computed solution on $2N, 2M$ number of mesh points. The parameter uniform error is calculated using the formula $E^{N,M} = \max_{\varepsilon,\delta,\eta} \left(E_{\varepsilon,\delta,\eta}^{N,M}\right)$. The rate of convergence of the

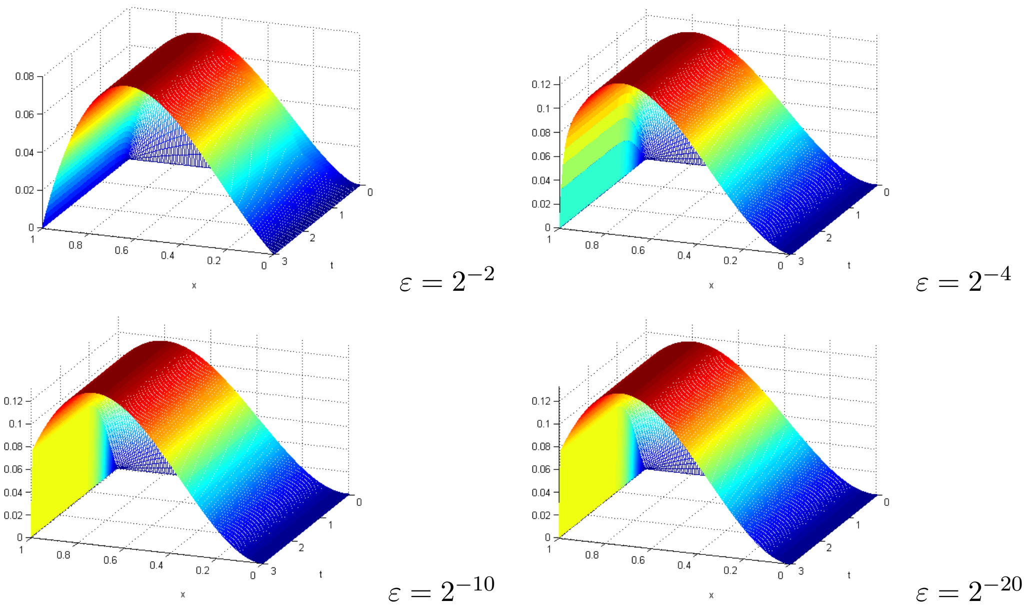

FIGURE 2. Boundary layer formation of the computed solution of Example 4.2.

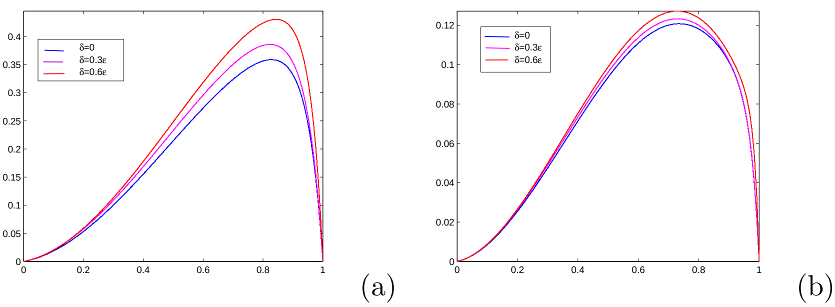

FIGURE 3. Plot of the solution for different δ at $T = 3$, $\varepsilon = 2^{-2}$ and $\eta = 0.5\varepsilon$: (a) Example 4.1, (b) Example 4.2.

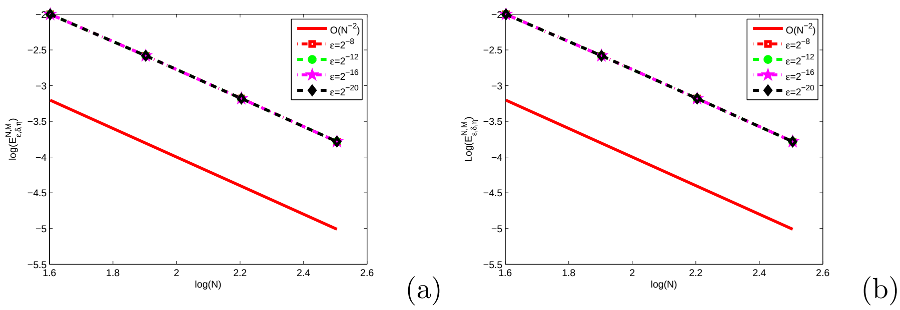

FIGURE 4. $E^{N,M}_{\varepsilon,\delta,\eta}$ for different values of ε in Log-Log scale: (a) Example 4.1; (b) Example 4.2.

scheme is calculated using $r^{N,M}_{\varepsilon,\delta,\eta} = \log_2\left(E^{N,M}_{\varepsilon,\delta,\eta}\right) - \log_2\left(E^{2N,2M}_{\varepsilon,\delta,\eta}\right)$ and the parameter uniform rate of convergence is calculated using $r^{N,M} = \log_2\left(E^{N,M}\right) - \log_2\left(E^{2N,2M}\right)$.

TABLE 1. Maximum absolute errors for different values of ε, when $\theta = 0.5$, $\delta = 0.6\varepsilon$ and $\eta = 0.5\varepsilon$.

$\varepsilon \downarrow$	$M = 10$	20	40	80
	$N = 16$	32	64	128
Example 4.1				
2^{0}	1.9351e-04	1.5643e-05	1.8560e-06	3.3466e-07
2^{-2}	4.3093e-03	3.3172e-04	4.0187e-05	9.4034e-06
2^{-4}	5.3093e-03	2.5607e-03	2.9779e-04	2.1417e-05
2^{-6}	6.3093e-03	2.6382e-03	6.6378e-04	1.5892e-04
2^{-8}	9.9812e-03	2.6266e-03	6.6078e-04	1.6505e-04
2^{-10}	9.9711e-03	2.6237e-03	6.6004e-04	1.6486e-04
2^{-12}	9.9686e-03	2.6229e-03	6.5985e-04	1.6482e-04
2^{-14}	9.9680e-03	2.6228e-03	6.5980e-04	1.6480e-04
2^{-16}	9.9678e-03	2.6227e-03	6.5979e-04	1.6480e-04
2^{-18}	9.9678e-03	2.6227e-03	6.5979e-04	1.6480e-04
2^{-20}	9.9678e-03	2.6227e-03	6.5979e-04	1.6480e-04
$E^{N,M}$	9.9678e-03	2.6227e-03	6.5979e-04	1.6480e-04
$r^{N,M}$	1.9262	1.9910	2.0013	-
Example 4.2				
2^{0}	1.1217e-04	6.7657e-06	4.0253e-07	2.5099e-08
2^{-2}	2.8214e-03	2.2853e-04	1.4596e-05	9.1374e-07
2^{-4}	3.9041e-03	1.0977e-03	1.9762e-04	1.5232e-05
2^{-6}	3.9008e-03	1.0958e-03	2.7899e-04	7.0010e-05
2^{-8}	3.9997e-03	1.0948e-03	2.7881e-04	7.0091e-05
2^{-10}	3.9994e-03	1.0945e-03	2.7876e-04	7.0080e-05
2^{-12}	3.9994e-03	1.0945e-03	2.7875e-04	7.0077e-05
2^{-14}	3.9994e-03	1.0945e-03	2.7875e-04	7.0076e-05
2^{-16}	3.9994e-03	1.0945e-03	2.7875e-04	7.0076e-05
2^{-18}	3.9994e-03	1.0945e-03	2.7875e-04	7.0076e-05
2^{-20}	3.9994e-03	1.0945e-03	2.7875e-04	7.0076e-05
$E^{N,M}$	3.9994e-03	1.0945e-03	2.7875e-04	7.0076e-05
$r^{N,M}$	1.8695	1.9732	1.9920	-

5. Discussion and conclusion

In this paper we have considered a numerical scheme to solve a time-dependent singularly perturbed differential difference equation which provides higher order convergence in space based on extrapolation method. First, using Taylor's series approximation for the terms with the shift parameters, we convert the equation into singularly perturbed time dependent differential equation. The numerical scheme is developed using θ-method for temporal discretization and the exponential fitted central finite difference method for spatial discretization by inducing the exponential fitting parameter. The existence of unique discrete solution are discussed. The proposed discrete scheme is stable for all values of the perturbation parameter. The parameter uniform convergence of the scheme is proved and discussed. Numerical examples that exhibits a boundary layer behaviour are considered for validating the theoretical analysis. The approximate solution is computed for different

Table 2. Example 4.1, comparison of the proposed scheme with different schemes in the literatures.

Numerical Schemes		$M = 60$	120	240	480
$\downarrow$		$N = 32$	64	128	256
Proposed Scheme	$E^{N,M}$	2.1274e-03	5.5403e-04	1.3996e-04	3.5081e-05
	$r^{N,M}$	1.9411	1.9849	1.9963	1.9992
Upwind Scheme in [23]	$E^{N,M}$	1.6716e-02	9.2021e-03	4.9863e-03	2.6885e-03
	$r^{N,M}$	0.8612	0.8840	0.8912	0.9163
Mid-Pt Scheme in [23]	$E^{N,M}$	1.0729e-02	6.5942e-03	3.8199e-03	2.1180e-03
	$r^{N,M}$	0.7022	0.7877	0.8508	0.8938
Result in [24]	$E^{N,M}$	6.0781e-03	3.3107e-03	1.7254e-03	8.8049e-04
	$r^{N,M}$	0.8765	0.9402	0.9705	0.9854
Result in [14]	$E^{N,M}$	7.5020e-03	4.4966e-03	2.4450e-03	1.2728e-03
	$r^{N,M}$	0.7384	0.8791	0.9418	0.9715
Result in [32]	$E^{N,M}$	9.7515e-03	4.8801e-03	2.4414e-03	1.2211e-03
	$r^{N,M}$	0.9987	0.9992	0.9995	0.9998

Table 3. Example 4.2, comparison of the proposed scheme with different schemes in literatures.

Numerical Schemes		$M = 30$	60	120	240
$\downarrow$		$N = 16$	32	64	128
Proposed Scheme	$E^{N,M}$	3.9857e-03	1.0928e-03	2.7895e-04	7.0101e-05
	$r^{N,M}$	1.8668	1.9700	1.9925	1.9985
Result in [14]	$E^{N,M}$	1.5241e-02	7.6388e-03	3.8384e-03	1.9277e-03
	$r^{N,M}$	0.9924	0.9925	0.9925	0.9964
Result in [32]	$E^{N,M}$	9.3302e-03	5.8132e-03	3.1997e-03	1.6737e-03
	$r^{N,M}$	0.6826	0.8614	0.9349	0.9685

values of the perturbation parameter ε ranging from $\varepsilon = 1$ to $\varepsilon = 2^{-20}$. In the computation we consider for the shift parameters $\delta < \varepsilon$ and $\eta < \varepsilon$.

In Figure 1 and 2, we depicted the computed solution of Example 4.1 and 4.2 for different values of ε. In these figures, we observe the formation of the boundary layer as ε goes small. Effect of the shift parameters on the behaviour of the solution is depicted in Figure 3. If the negative shift parameter grows in magnitude, then the thickness of the boundary layer decreases as it is observed in Figure 3 (a) and (b). In Table 1, the maximum absolute error and the parameter uniform error of Example 4.1 and 4.2 are given. The result in this table shows that as the perturbation parameter goes small the maximum absolute error becomes the same after some steps. In Table 4, the maximum absolute error for different values of the shift parameters are given. In Figure 4, one can observes that, while the perturbation parameter goes small the scheme converges uniformly. The Log-Log scale plot of the maximum absolute error are consistently overlapped. From the results in Table 4, one can observe that, the scheme is more accurate than the methods given in [14], [23], [24] and [32].

TABLE 4. Maximum absolute error for different values of δ and η at $\varepsilon = 2^{-2}$.

	$M = 10$	20	40	80
	$N = 16$	32	64	128
Example 4.1				
$\delta \downarrow$	$\eta = 0.5\varepsilon$			
$\delta = 0.1\varepsilon$	3.0426e-03	2.3557e-04	3.1642e-05	7.1983e-06
$\delta = 0.3\varepsilon$	3.1868e-03	2.4904e-04	3.3850e-05	7.7893e-06
$\delta = 0.5\varepsilon$	3.7279e-03	2.8918e-04	3.7416e-05	8.7171e-06
$\delta = 0.7\varepsilon$	5.3742e-03	4.1372e-04	4.4420e-05	1.0313e-05
$\eta \downarrow$	$\delta = 0.6\varepsilon$			
$\eta = 0.1\varepsilon$	3.3199e-03	2.6883e-04	3.7449e-05	8.6710e-06
$\eta = 0.3\varepsilon$	3.6655e-03	2.8969e-04	3.8649e-05	9.0041e-06
$\delta = 0.5\varepsilon$	4.3093e-03	3.3172e-04	4.0187e-05	9.4034e-06
$\eta = 0.7\varepsilon$	5.5191e-03	4.2326e-04	4.2410e-05	9.7502e-06
Example 4.2				
$\delta \downarrow$	$\eta = 0.5\varepsilon$			
$\delta = 0.1\varepsilon$	1.6384e-03	1.1198e-04	7.0679e-06	4.4195e-07
$\delta = 0.3\varepsilon$	1.7780e-03	1.2264e-04	7.7278e-06	4.8322e-07
$\delta = 0.5\varepsilon$	2.2951e-03	1.6710e-04	1.0607e-05	6.6346e-07
$\delta = 0.7\varepsilon$	3.5850e-03	4.0970e-04	2.7232e-05	1.7099e-06
$\eta \downarrow$	$\delta = 0.6\varepsilon$			
$\eta = 0.1\varepsilon$	8.9646e-04	5.9853e-05	3.7500e-06	2.3381e-07
$\eta = 0.3\varepsilon$	1.4146e-03	9.5324e-05	5.9960e-06	3.7481e-07
$\delta = 0.5\varepsilon$	2.8214e-03	2.2853e-04	1.4596e-05	9.1374e-07
$\eta = 0.7\varepsilon$	3.8849e-03	5.9304e-04	4.1714e-05	2.6315e-06

Acknowledgement. The author thanks the referees for their constructive comments and corrections.

References

[1] Bansal, K., Sharma, K. K., (2016), ε-Uniform numerical technique for the class of time dependent singularly perturbed parabolic problems with state dependent retarded argument arising from generalised Stein's model of neuronal variability, Differ. Equ. Dyn. Syst., 2016, 1-28.

[2] Bansal, K., Sharma, K. K., (2017), Parameter uniform numerical scheme for time dependent singularly perturbed convection-diffusion-reaction problems with general shift arguments, Numer. Algorithms, 75, 113-145.

[3] Bansal, K., Rai, P., Sharma, K. K., (2017), Numerical treatment for the class of time dependent singularly perturbed parabolic problems with general shift arguments, Differ. Equ. Dyn. Syst., 25, 327-346.

[4] Clavero, C., Gracia, J. L., Jorge, J. C., (2005), High-order numerical methods for one-dimensional parabolic singularly perturbed problems with regular layers, Numer. Methods Partial Differential Equations, 21, 149-169.

[5] Chandru, M., Prabha, T., Das, P., Shanthi, V., (2019), A numerical method for solving boundary and interior layers dominated parabolic problems with discontinuous convection coefficient and source terms, Differ. Equ. Dyn. Syst. 27(1), 91-112.

[6] Chandru, M., Das, P., Ramos, H., (2018), Numerical treatment of two parameter singularly perturbed parabolic convection diffusion problems with non-smooth data, Mathematical Methods in the Applied Sciences, 41(14), 5359-5387.

[7] Das, P., (2018), A higher order difference method for singularly perturbed parabolic partial differential equations, Journal of Difference Equations and Applications, 24(3), 452-477.

[8] Das, P., Natesan, S, (2013), Richardson extrapolation method for singularly perturbed convection-diffusion problems on adaptively generated mesh, Comput. Model. Eng. Sci, 90, 463-85.

[9] Das, P., Rana, S., Vigo-Aguiar, J., (2020), Higher order accurate approximations on equidistributed meshes for boundary layer originated mixed type reaction diffusion systems with multiple scale nature, Applied numerical mathematics, 148, 79-97.

[10] Das, P., (2015), Comparison of a priori and a posteriori meshes for singularly perturbed nonlinear parameterized problems, Journal of computational and applied mathematics, 290, 16-25.

[11] Das, P., Vigo-Aguiar, J., (2019), Parameter uniform optimal order numerical approximation of a class of singularly perturbed system of reaction diffusion problems involving a small perturbation parameter, Journal of Computational and Applied Mathematics, 354, 533-544.

[12] Doolan, E. P., Miller, J. J., Schilders, W. H., (1980), Uniform numerical methods for problems with initial and boundary layers, Boole Press, Dublin.

[13] Gupta, V., Kumar, M., Kumar, S., (2018), Higher order numerical approximation for time dependent singularly perturbed differential-difference convection-diffusion equations, Numer. Methods Partial Differential Equations, 34, 357-380

[14] Kumar, D., Kadalbajoo, M. M., (2011), A parameter-uniform numerical method for time-dependent singularly perturbed differential-difference equations, Appl. Math. Model., 35, 2805-2819

[15] Kumar, S., Kumar, R., (2017), A domain decomposition Taylor Galerkin finite element approximation of a parabolic singularly perturbed differential equation, Appl. Math. Comput., 293, 508-522

[16] Kumar, S., Kumar, R., (2017), A finite element domain decomposition approximation for a semi-linear parabolic singularly perturbed differential equation, Int. J. Nonlinear Sci. Numer. Simul., 18, 41-55

[17] Kumar, S., Kumar, R., (2015), Convergence of three-step Taylor Galerkin finite element scheme based monotone schwarz iterative method for singularly perturbed differential-difference equation, Numer. Funct. Anal. Optim., 36(8), 1029-1045

[18] Kumar, K., Podila, P. C., Das, P., Ramos, H., (2021), A graded mesh refinement approach for boundary layer originated singularly perturbed time delayed parabolic convection diffusion problems, Mathematical Methods in the Applied Sciences, 44(16), 12332-12350.

[19] Lange, C. G., Miura, R. M., (1985), Singular perturbation analysis of boundary value problems for differential-difference equations III. Turning point problems, J. Appl. Math., 45, 708-734.

[20] Lange, C. G., Miura, R. M., (1994), Singular perturbation analysis of boundary value problems for differential-difference equations. V. Small shifts with layer behavior, J. Appl. Math., 54, 249-272

[21] Linß, T., (2009), Layer adapted meshes for reaction convection diffusion problems, Springer.

[22] O'Malley, R. E., (1991), Singular perturbation methods for ordinary differential equations, Springer.

[23] Ramesh, V. P., Kadalbajoo, M. K., (2008), Upwind and mid-point upwind difference methods for time dependent differential difference equations with layer behaviour, Appl. Math. Comput., 202, 453-471.

[24] Rao, R. N., Chakravarthy, P. P., (2017), Fitted numerical methods for singularly perturbed 1D parabolic partial differential equations with small shifts arising in the modeling of Neuronal variability, Differ. Equ. Dyn. Syst., 2017, 1-18

[25] Roos, H. G., Stynes, M., Tobiska, L. R., (2008), Numerical methods for singularly perturbed differential equations, Springer Science & Business Media.

[26] Shakti, D., Mohapatra, J., Das, P., Vigo-Aguiar, J., (2022), A moving mesh refinement based optimal accurate uniformly convergent computational method for a parabolic system of boundary layer originated reaction–diffusion problems with arbitrary small diffusion terms, Journal of Computational and Applied Mathematics, 404, 113167.

[27] Shishkin, G. I., Shishkina, L. P., (2008), Difference methods for singular perturbation problems, CRC Press.

[28] Smith, G. D., (1985), Numerical solution of partial differential equations: Finite difference methods, Oxford University Press.

[29] Tian, H., (2002), The exponential asymptotic stability of singularly perturbed delay differential equations with a bounded lag, J. Math. Anal. Appl., 270, 143-149.

[30] Woldaregay, M. M., Duressa, G. F., (2020), Higher-order uniformly convergent numerical scheme for singularly perturbed differential difference equations with mixed small shifts, International Journal of Differential Equations, (2020), 1-15.

[31] Woldaregay, M. M., Aniley, W. T., Duressa, G. F., (2021), Novel Numerical Scheme for Singularly Perturbed Time Delay Convection-Diffusion Equation, Advances in Mathematical Physics, 2021, 1-13.

[32] Woldaregay, M. M., Duressa, G. F., (2020), Uniformly convergent numerical scheme for singularly perturbed parabolic delay differential equations, ITM Web of Conferences, 34, EDP Sciences.

[33] Woldaregay, M. M., Duressa, G. F., (2022), Fitted numerical scheme for solving singularly perturbed parabolic delay partial differential equations, Tamkang J. of Mathematics, 53, In press.

Mesfin Mekuria Woldaregay received his BEd degree in Mathematics from Jimma University in 2006; MSc degree in Mathematics from Addis Ababa University in 2010 and PhD degree in Mathematics from Jimma University in 2021. Currently, he is an Assistant Professor of Mathematics in the Department of Applied Mathematics, Adama Science and Technology University. His research interest includes numerical solution of singularly perturbed problems.